Stony Brook University

Meteorological Factors Affecting Storm Surge of Extra Tropical Cyclones along the New York/New Jersey Coast

A Thesis Presented

by

Aichen Niu

to

The Graduate School

in Partial Fulfillment of the

Requirements

for the Degree of

Master of Science

in

Marine and Atmospheric Science

Stony Brook University

May 2015

Stony Brook University

The Graduate School

Aichen Niu

We, the thesis committee for the above candidate for the

Master of Science degree, hereby recommend

acceptance of this thesis.

Sultan Hameed – Thesis Advisor
Professor, School of Marine & Atmospheric Sciences

Brian Colle – Second Reader
Professor, School of Marine & Atmospheric Sciences

Edmund K.M. Chang– Third Reader
Professor, School of Marine & Atmospheric Sciences

This thesis is accepted by the Graduate School

Charles Taber
Dean of the Graduate School

Abstract of the Thesis

Meteorological Factors Affecting Storm Surge of Extra Tropical Cyclones along the New York/New Jersey Coast

by

Aichen Niu

Master of Science

in

Marine and Atmospheric Science

Stony Brook University

2015

Abstract:

Storm surge is an abnormal rise or decrease of water generated by a storm, over and above the predicted astronomical tide. It is a rise of coastal shallow water driven by a storm's surface wind and pressure gradient forces. There are at least four processes involved in altering tide levels during storms: the pressure effect, the direct wind effect, the effect of waves, and the rainfall effect. Extra-tropical storms cause an offshore rise of water. Unlike most tropical cyclone storm surge, extra-tropical storms can cause higher water levels across a large area for longer periods and can lead to significant coastal flooding.

The most common application of joint probability methods in coastal engineering is to waves and sea levels occurring near high tide for assessment of flood risk at sea defences. For the purposes of the JPM method, the storm is described in terms of its characteristics at or near landfall, using the following parameters: pressure deficit ΔP, radius of the exponential pressure profile R_p, Holland's B parameter, forward velocity V_f, storm heading θ, and the landfall location. The objective of this

study is to provide a basis for the application of the JPM method to assess the impact of extra tropical storms in the NY-NJ coastal region by investigating possible meteorological properties of storms that can affect the storm surge. The following factors were studied in a region east of Battery where the surge is optimally related to storm properties: storm velocity, acceleration, orientation of storms, the minimum pressure, distance from storm center to the Battery, and the analysis of impacts of wind velocity, wind stress at The Battery on storm surge. Correlations between storm properties and surge suggest that storm velocity and minimum central pressure have significant impact on surge and lower velocity or minimum central pressure correspond to higher surge. However, there is no evidence that acceleration and distance from storm center to The Battery have significant impact on surge. Most storms are moving 20-40 degree with respect to the East to the Northeast. Storms with angles ranging from -45 degree to 40 degree have significant impact on surge. An extreme value analysis of minimum pressure and maximum storm surge was also carried out. An approximation of the return period of Hurricane Sandy from the extreme value analysis is about 550 years.

Table of Contents

List of Tables

List of Figures

Acknowledgments

I offer my sincere appreciation for the learning opportunities with my advisor, Professor Sultan Hameed. I would like to thank the committee members, Professor Edmund Chang and Professor Brian Colle. Thank you for reading my thesis proposal and giving me suggestions.

I have special thanks to Keith Roberts. Thank you for sharing the data and helping me pair the cyclone features with the surge record at The Battery and plot the data. I thank Albert Yau for sharing the NCEP data with me.

Finally, I would like to thank Minghua Zheng, Parama Mukherjee and Zhenhai Zhang. Thank you for helping me with course works during these two years at Somas.

Chapter 1: Introduction

By definition, storm surge is an abnormal rise or decrease of seawater generated by a storm, over and above the predicted astronomical tide. “It is a rise of coastal shallow water driven by a storm's surface wind and pressure gradient forces, produced by water being pushed toward the shore by the force of the winds moving cyclonically around the storm and lower central pressure associated with the storm causes the ocean to rise” (National Hurricane Center). Storm surge can be negative. Negative storm surge occurs when the wind direction blows the water away from the coast and causes the water level to decrease (Chanson, 2004). In reality, storm surge does not include all factors that cause water levels to rise along the coast during a hurricane. Waves and freshwater input can also raise water levels. Breaking waves raise the water levels through wave runup and wave setup. They occur “when a wave breaks and the water is propelled onto the beach and when waves continually break onshore and the water from the runup piles up along the coast” (National Hurricane Center). Heavy rainfall ahead of a hurricane can cause river levels to rise well inland from the coast. Thus, freshwater can also raise water levels, especially near deltas and in bays (National Hurricane Center).

The mechanism of storm surge can be described as four processes associated with the passage of a storm, which can alter the water level: the pressure effect, the direct wind effect, the effect of waves, and the rainfall effect (Harris, 1963). Water level rises under low pressure because of the hydrostatic process. The density of waterρequals to 103 kg/ m3, and the pressure exerted by water equals to ρ g ħ, where g is the gravity acceleration which equals to 9.8m/s2 and h is the height that water level will rise. Suppose the pressure dropped equals to 10 hPa. Then the height that water level will rise equals to pressure divided by gravity acceleration times water density which equals to 10 centimeter. The second process is the direct wind effect. There are

two types of direct wind effects. The first type of wind effect mentioned by Harris is that strong surface winds cause surface currents at a 45 degree angle to the wind direction. This phenomenon is known as the Ekman Spiral. The second type of wind effect is known as wind stress which causes water level to increase at the downwind shore and to decrease at the upwind shore. The next process is the effect of waves. Powered by the wind, the effect of waves is distinct from a storm's wind-powered currents (Harris, 1963). In this process, in the direction that it moves, powerful wind will whips up large and strong waves. These surface waves are responsible for very little water transport in open water, but they may cause significant water transport near the shore. When waves are breaking on a line or parallel to the beach, they can carry considerable water toward the shore. "As they break, water particles moving shoreward have considerable momentum and may run up a sloping beach to an elevation above the mean water line which may exceed twice the wave height before breaking" (Granthem, 1953). The next process is the rainfall effect which is experienced in estuaries. Hurricanes may cause up to 12 inches of rainfall in one day over large areas. Heavy rainfalls will result in quick rise in water levels of rivers (Harris, 1963).

New York City and its adjacent regions such as northern New Jersey and Long Island, New York, are strongly influenced by tides and weather. "Much of the Metropolitan region is less than 5 m above mean sea level (MSL), with about 260 km2 at risk from storm surge flooding by a 100-yr flood event for both tropical systems and nor'easter cyclones" (Bowman et al. 2005). One major cause of hurricane damage is storm surge. Water levels at Battery Park peaked at ~2.5 m (8 ft) above MSL during the December 1992 nor'easter event. "Sea level overtopped the city's seawalls for only a few hours, but this was enough to flood the NYC subway and the Port Authority Trans-Hudson Corporation (PATH) train systems at the Hoboken train station in New

Jersey, thus precipitating a shutdown of these transportation systems for several days" (Colle et al., 2008). In 2012, the estimated damage caused by Hurricane Sandy was near $50 billion, making it the second-costliest cyclone to hit the United States since 1900 (Blake et al., 2013). Storm surge is seen as the greatest threat to human's life and property along the coast. Thus, predict storm surge and coastal flooding accurately is very essential for developing cost effective storm mitigation and preparation (Sheng et.al, 2010).

Joint Probability Method (JPM) is usually used in the flood risk calculations. The Joint-Probability Method for evaluating surges in sea level associated with tropical storms and its application to the NY-NJ area is described by Resio (2007) and Toro et al. (2010). These studies are built upon the experience from the Mississippi Surge study (FEMA, 2008; Niedoroda et al., 2010) with the appropriate data and model modifications to capture the conditions in NY-NJ. In these studies, meteorological characteristics of tropical storms at or near landfall are used as the primary variables. These studies justify the following two arguments: (1) "most of the coastal surge is generated by the storm in the last 90 nautical miles prior to landfall" (Resio, 2007), and (2) there are more and better hurricane data available at the coast compare to offshore, especially for older storms.

"Joint probability analysis gives the probability of the relevant variables taking high values simultaneously and thus creating a situation where flooding may occur. The most common application of joint probability methods in coastal engineering is to waves and sea levels occurring near high tide for assessment of flood risk at sea defences" (Hawks, 2005). Another application of the JPM is the estimation of storm surge elevation frequencies. Pioneered by pioneered by Myers (Myers 1975, Ho and Myers 1975), JPM is one of the approaches for this

task for coastal flood estimation. In recent years, it has been recognized that JPM is preferred for the tropical storm environment among available methods (FEMA, 2012).

FEMA (2008) developed a probabilistic model to represent the occurrence rate and characteristics of future hurricanes capable of producing significant surge inundation along the Mississippi coast. This study provided two inputs for a Mississippi storm surge study performed by the URS Group: "A probabilistic characterization of the occurrence and characteristics of future hurricanes that may cause significant surge along the Mississippi coast" (FEMA, 2008) and a set of representative synthetic storms generated by means of a JPM-OS scheme.

The JPM method describes storm in terms of its characteristics at or near landfall, using the parameters such as: pressure deficit P which represents hurricane intensity, radius of the exponential pressure profile $p\ R$ which represents hurricane size, Holland's B parameter which controls the shape of the pressure and wind fields, forward velocity $f\ V$, storm heading , and the landfall location which represents the minimum distance from the track to a reference point along the coast (FEMA, 2008). These parameters are illustrated in Figure 1. They represent the main hurricane parameters affecting storm surge and are treated as random variables in the JPM method explicitly (FEMA, 2008).

"The JPM method considers all possible combinations of storm characteristics at landfall, with their associated probabilities, calculates the surge effects for each combination" (FEMA, 2008). The JPM combines these results to obtain the annual probability of exceeding any storm surge that desired by researchers (FEMA, 2008). The results obtained in this thesis suggest that storms that generate a surge at The Battery, New York are over the elliptical regions shown in Figure 2. However, it is highly inefficient to use the JPM approach in conjunction with the modern generation of complex high-resolution numerical models (FEMA, 2008). To solve this

problem, FEMA (2008) introduced “a new approach to the selection of the storm simulation set that permits reduction of the JPM computational effort”. Their method uses an integration scheme called Bayesian quadrature to “evaluate the multidimensional joint probability integral over the space of storm parameters as weighted summation over a relatively small set of optimally selected nodes (synthetic storms)” (Toro, 2010). They simulate a set of representative “Synthetic Storms” and the corresponded recurrence rates. These synthetic storms have characteristics such as starting times for the purpose of astronomical-tide calculations, and recurrence rates that make them representative of the entire possible future storms. They then use these rates for the numerical wind, wave, and surge final probability calculations (Toro, 2010).

Extratropical storms cause an offshore rise of water. “Unlike tropical storms, extratopical storms can cause higher water levels across a larger area for longer periods” (mahalo.com). In current practice, the occurrence and surge effects of extra-tropical storms are not modeled with the JPM approach described above. The objective of this study was to provide a basis for the application of the JPM method to assess the impact of extra tropical storms in the NY-NJ coastal region. The climatology of storm surge in this region is presented by Colle et.al. (2010). The main purpose of this work was to identify meteorological properties of storms that can affect the storm surge. For this purpose, I investigated storms in the historical data base, using the climate forecast system reanalysis (CFSR; Saha et al. 2010) data from 1979-2005, November to March. The following factors were studied: storm velocity, acceleration, orientation of storms and the minimum pressure. In addition to the CFSR 1979-2005 data, I use the same methodology to analyze a longer dataset which is the NCEP- NCAR reanalysis data from 1948-2012, October to March. Statistical properties of these variables are described in Sections 3~10. The correlation coefficients between storm surge at Battery Park, New York and storm properties are calculated,

shown in Table 1b. Correlations obtained from the 1979-2005 period are shown in Table 1a. Statistically significant correlations are shown in bold. Section 7 gives the extreme-value analysis on maximum storm surge and minimum pressure. The 100-year return periods of maximum storm surge and minimum pressure are calculated to estimate the probability of an unusually large event.

In addition, the distance between storm center and The Battery is considered as a possible variable which impacts storm surge. The verification of this assumption is documented in Section 8. Section 9 documents the correlation between u and v winds and corresponding stress and storm surge. The wind data used in this section is the NCEP-NCAR reanalysis data from 1948-2012.

Chapter 2: Data and Methods

"Extratropical cyclones are responsible for much of the high impact weather in the mid-latitudes and high latitudes during the cool season, including coastal storm surges" (Colle et al., 2008). The data used was the climate forecast system reanalysis (CFSR; Saha et al. 2010) at ~38km grid spacing from 1979 to 2005, November to March. Cyclone tracks were constructed using 6-hourly sea level pressure from the CFSR. The two criteria used for the automated tracking cyclones include at least one 2 hPa closed MSLP contour to be counted manually, and the storm had to persist for at least 24-h and move at least 1000km (Colle et.al, 2013). The surface cyclone tracking algorithm is developed by Hodges (1994, 1995).

The second data set used in this study includes all cyclones between 1948 and 2012 from October to March using the 2.5 x 2.5 NCEP-NCAR reanalysis data. Hodges (1999) gives an algorithm for tracking negative SLP anomaly centers. In this algorithm, all negative SLP minima

are identified at each time step and linked together across time steps to form cyclone tracks using constraints on track smoothness and maximum displacement distance. To track cyclones, a minimum in SLP should be defined. In this case, the negative minima in p' is tracked, with p' defined as p'= p-1020 (in hPa). That is, for this dataset, all cyclones with central pressure below 1020 hPa are tracked. All cyclones between 1948 and 2012 from October to March have been tracked using the 2.5x2.5 NCEP-NCAR reanalysis data. This data was paired with Battery Park's surge record. The black box in Figure 2a contains all cyclones that generate surge and the elliptical regions shown in Figure 2b contain 95% of all cyclone features that generate the surge at The Battery. Cyclone features were time-matched to storm surge time series data at The Battery and assumed the cyclone features follow normal distributions. From that, the analysis was restricted to only cyclone features that occurred with greater than or equal to a surge threshold at The Battery. These restricted data cyclone features have longitude and latitude data associated with them. To find the major and minor axis of the ellipse, the two standard deviations in longitude and latitude of this restricted cyclone track data are calculated. There are 2688 storms in total, 1366 storms in the blue ellipse and 1532 storms in the red ellipse. When calculating the storm velocity and storm acceleration in the blue and red ellipses, some storms are eliminated because they only have one or two locations in the elliptical regions.

Figure 2b shows the major surge regions as ellipses in different colors. Each line in Figure 2b indicates the track of a cyclone. The cyclone tracks are composed of cyclone features, and the surge data at Battery is time-matched to these cyclone features. The cyclone features that occur when there is a certain level surge are then averaged and this produces the center of the ellipse. The cyclone tracks are each composed of at least 4 cyclone features, which contain the time, latitude, longitude, and MSLP of the cyclone. The color-code in the legend indicates the

elliptical regions containing 95% of storm tracks associated with the surge at The Battery greater than or equal to the stated percentile of the surges. Specifically, 0.61m is the 99.5th percentile of the surges. In the blue ellipse, 95% of the storm tracks generate surge at that level. 0.51m is the 99th percentile of the surges. In the red ellipse, 95% of the storm tracks generate surge at that level. The calculation documented from Section 3 to Section 10 is based on the data in blue and red ellipses.

Chapter 3: Results and Discussion

a) Correlation between Pressure and Storm Surge

The correlation coefficient between the minimum central pressure of storms and corresponding storm surges is calculated. The correlation coefficients between pressure and storm surge for the blue ellipse and the red ellipse equal to -0.39 and -0.36, respectively. A significance test shows that both correlations are statistically significant at 1% level. The results obtained from CFSR data were -0.24 and -0.22. The values obtained from CFSR data were slightly smaller, but still statistically significant at 1% level. Therefore, minimum central pressure and storm surge are negative correlated and lower minimum pressure corresponds to higher storm surge. This conclusion can be interpreted as inverted barometer effect that a 1 hPa decrease of atmospheric pressure below a reference pressure cause a 1 cm increase in water level (Kantha et.al, 1994).

b) Calculation of Storm Velocities

To examine how fast the cyclones move inside the elliptical regions, velocities of cyclones are calculated. For a cyclone inside the defined region, with latitude and longitude data at each 6th hour, the geodistance from its initial location to its final location in the ellipse is calculated.

By dividing the geodistance by the time that the cyclone moves inside the elliptical region, we can get the velocity of the cyclone. The average velocities in the blue ellipse and the red ellipse are 15.3 m/s and 15.3 m/s, respectively. The values obtained from CFSR data were 14.5 m/s and 15.0 m/s, respectively. Results are fairly the same.

The velocity results are shown as histograms (Figure 3a and 3b) and fitted into Gaussian and Gamma distributions (Figure 3c and 3d). The histogram is a common graphical way to plot a single batch of data. The range of a batch of data is divided into bins and the number of values falling into each bin is counted (Wilks, 2011). When choosing the bin width of a histogram, if the intervals are too wide, the histogram will be too smooth, which means some important details of the data will be missed. If the intervals that are too narrow, the plot will be too rough and difficult to interpret (Wilks, 2011). Wilks (2011) gave a formula to determine the binwidth, h by computing

$$h \approx \frac{c\,IQR}{n^{\frac{1}{3}}}.$$

In this formula, c is a constant ranging from 2.0~2.6, n is the number of elements in this single batch of data, and IQR is the interquartile range which is the difference between the upper and lower quartiles. The c value used in this study is 2.2.

Figure 3c and 3d show the probability density distribution of velocity and its fitting into Gaussian and Gamma distribution using the method of maximum likelihood. Figure 3c shows storm velocities in the blue ellipse fitted to normal distribution with $\mu = 15.29$ and $\sigma = 5.98$, and Gamma distribution with $\alpha = 5.99$ and $\beta = 2.55$. Results obtained from CFSR data were $\mu = 14.54$, $\sigma = 6.35$ and $\alpha = 5.31$, $\beta = 2.74$. Figure 3d shows storm velocities in the red ellipse fitted into normal distribution with $\mu = 15.30$ and $\sigma = 5.84$, and Gamma distribution with $\alpha = 6.23$ and $\beta = 2.45$. Results obtained from CFSR data were $\mu = 14.86$, $\sigma = 5.82$, and $\alpha = 6.08$ and $\beta = 2.4$. The

one-sample Komogorov-Smirnov (K-S) test is presented to test the goodness of fit of Gaussian and Gamma distribution. The null hypothesis of the K-S test is that the velocity data is drawn from the fitted Gaussian or Gamma distribution. For both ellipses, the K-S test indicates that the null hypothesis should be rejected which means both Gaussian and Gamma distributions do not fit the velocity well. However, Figure 3e and 3f show that the difference between theoretical cumulative distribution function and fitted cumulative distribution function of Gamma distribution is smaller than that of Gaussian distribution, thus we can conclude that Gamma distribution is a better fitting for the velocity of both ellipses. This result is also consistent with the result obtained from CFSR data.

The correlation between storm surge and velocity of blue ellipse is -0.31, and a significance test shows that this correlation coefficient is statistically significant at the 1% level. For the red ellipse, the correlation coefficient is -0.22 which also shows the correlation is statistically significant at 1% level. Correlations obtained from CFSR data, shown in Table 1a, were -0.32 and -0.27 which also significant at 1% level. Correlation coefficients with statistical significance are shown in bold in Table 1b. Above results indicate that higher storm velocity corresponds to lower storm surge. The interpretation of this conclusion is that if the storm moves faster, the wind has less time to force the water. Also, the effective v wind to the left of the storm (in the coastal region) becomes weaker. This makes the surge less if the storm moves faster.

c) Calculation of Storm Acceleration

The previous Section shows the effect of storm velocity on storm surge. It is also interesting to study the change of velocity, that is the acceleration, and see how it affects storm surge. Likewise, results are also shown as histograms (Figure 4a and 4b). The selection of the binwidth h of histograms also follows the formula

$$h \approx \frac{cIQR}{n^{\frac{1}{3}}}.$$

Because some of the storms only have two points in the studied area, we are not able to calculate their accelerations. After eliminating storms with only two points, 961 storms remain in the blue ellipse and 1172 storms remain in the red ellipse.

The calculated accelerations are also fitted into Gaussian and Gamma distributions, shown in Figure 4c and 4d. For the blue ellipse, the acceleration data is fitted to Gaussian distribution with μ= 0.0034 and σ= 7.30x10-4, and Gamma distribution with α=1.64 and β= 2.05. Results obtained from CFSR data were μ= 0.001, σ= 2.21x10-4 and α=2.06, β= 4.85. For the red ellipse, the acceleration data is fitted to Gaussian distribution with μ= 0.0039 and σ= 6.93x10-4, and Gamma distribution with α=2.64 and β= 1.46. Results obtained from CFSR data were μ= 0.0015 σ= 2.16x10-4 and α=2.17, β= 4.61. The one-sample Komogorov-Smirnov (K-S) test shows both Gaussian and Gamma distribution should be rejected. The result is consistent with the result obtained from CFSR data.

Correlations between storm acceleration and storm surge are also calculated. For the blue ellipse, the correlation coefficient is -0.06 which shows no statistical significance at 5% significance level. For the red ellipse, the correlation coefficient is -0.08 which also shows no statistical significance. Correlations obtained from CFSR data shown in Table 1a were 0.03 and 0.15 which also showed that the correlations are not statistical significant. Thus, there is no evidence that storm acceleration has a significant impact on storm surge.

The calculated accelerations are separated into positive values and negative values. For the blue ellipse, the correlations between positive acceleration and storm surge r1 and the correlations between negative acceleration and storm surge r2 are equal to 0.12 and -0.19, respectively. For the red ellipse, r1=-0.11 and r2=0.14. These values are slightly larger than the

values obtained from CFSR data which were r1=0.04, r2=-0.04 for the blue ellipse and r1=-0.13 and r2=0.04 for the red ellipse, But all these correlations are still not statistically significant. This result suggests that acceleration of the storms does not have an impact on surge level at The Battery.

d) Orientation of Storms

The track of each storm is approximated by a straight line using linear regression between the longitude and latitude of the cyclone at each 6-hour time step, while the angle between the simulated line and horizontal axis is calculated. The coefficient of determination R2 of each regression fit is a statistical measure of how close the longitude and latitude data are to the fitted regression line. If R2 is too small, it means the line is not a good representation of the track. In this study, storms with R2 less than 0.75 are eliminated. The panels (a) and (b) of Figure 5 show the tracks of two eliminated storms. The blue stars in each panel are the storm location at each time step and the red line is the predicted orientation of storms. Panels (c) and (d) are the histograms of angles of the blue ellipse and red ellipse. From these two histograms, most storms are moving 20-40 degree with respect to the East to the Northeast.

Weisberg et.al, (2006) published a paper about hurricane storm surge simulations for Tampa Bay. In their paper, they investigated the storm surge generated at the Tampa Bay, Florida, vicinity and their sensitivities to point of landfall, direction and speed of approach, and intensity. They concluded that the surge is sensitive to the approach direction (Weisberg et.al, 2006). Following Weisberg and Zheng's work, I separate the calculated angles into several groups. In each group, the correlation between storm velocity obtained in Section 4 and corresponding storm surge is calculated. Results are shown in Table 2. Statistically significant correlations are

shown in bold. From Table 2, storms with angles ranging from -45- to 40 degree with respect to the East have significant impact on surge.

e) Extreme Value Analysis of Minimum Pressure and Maximum Storm Surge

"The statistics of extreme values is used to describe the behavior of the largest m values" (Wilks, 2011). A typical method of studying extreme-value data is to collect the annual maximum, or block maximum of any dataset. Regardless of the distribution from which the observations come from, the largest of m independent observations from a fixed distribution will follow a known distribution increasingly closely as m increases (Wilks, 2011). This is called the Extremal Types Theorem which is "the analog within the statistics of extremes of the Central Limit Theorem for the distribution of sums converging to the Gaussian distribution" (Wilks, 2011). The distribution toward the largest-of-m values converges is called the generalized extreme value distribution, with PDF

$$f(x)=\frac{1}{\beta}\left[1+\frac{\kappa(x-\zeta)}{\beta}\right]^{1-\frac{1}{\kappa}}\exp\left\{-\left[1+\frac{\kappa(x-\zeta)}{\beta}\right]^{-\frac{1}{\kappa}}\right\},\ 1+\frac{\kappa(x-\zeta)}{\beta}>0.$$

The minimum pressure observed in each year in any storm has been collected and fitted into extreme value distribution with β= 7.08, κ=-0.33, and ζ= 969.68. The maximum storm surge in each year has been collected and fitted into extreme value distribution with β=0.20, κ=-0.09, and ζ=0.72. ζ is the location parameter, β is the scale parameter and κ is the shape parameter. The PDF function can be integrated analytically, yielding the CDF

$$F(x)=\exp\left\{-\left[1+\frac{\kappa(x-\zeta)}{\beta}\right]^{-\frac{1}{\kappa}}\right\}$$

and the CDF can be "inverted to yield an explicit formula for the quantile function" (Wilks, 2011),

$$F^{-1}(p)=\zeta+\frac{\beta}{\kappa}\{[-\ln(p)]^{-\kappa}-1\}$$

Figure 6 shows the probability density function of minimum pressure and maximum storm surge and their fitting to extreme value distribution.

The result of extreme-value analysis summarizes the quantiles corresponding to large cumulative probabilities such as the event with an annual probability of 0.01 of being exceeded. It is impossible to estimate the direct empirical of these extreme quantiles unless n is large enough (Wilks, 2011). "A well-fitting extreme value distribution will provide an objective way to extrapolate to probabilities that may be larger than 1-1/n" (Wilks, 2011). These extreme probabilities define the average return periods as

$$R(x) = \frac{1}{\omega[1-F(x)]}$$

where is the average sampling frequency and F(x) is the cumulative probability function. In this case, for annual maximum or minimum data, =1 yr-1, and the event x corresponded to a cumulative probability F(x) will have a probability equals to 1-F(x) of being exceeded in any given year. The value of x associated with a return period of 100 years and would be called the 100-year event (Wilks, 2011). Figure 7 shows the 100-year return period of maximum storm surge (Figure 7a) and minimum storm pressure (Figure 7b). From Figure 7a, a reasonable estimate for the 100-year value of storm surge is calculated to be 1.91m, and a reasonable estimate for the 100-year value of minimum pressure is calculated to be 955.8 hPa. More specifically, if the surge of a certain storm is equal to 1.91m, this storm is said to be a 100-year event, and we expect this event to occur every 100 years. Likewise, if the minimum pressure of a certain storm is equal to 955.8 hPa, this storm is said to be a 100-year event, and we expect this event to occur every 100 years. The return periods calculated using CFSR data were 1.88m for the maximum surge and 958 hPa for the minimum pressure, which are very close to these results. The NOAA Water Level and Meteorological Data Report (Fanelli et al, 2013) provides the

information that the maximum storm surge of the hurricane Sandy measured at The Battery, New York was 2.86m. According to my calculation, hurricane Sandy is an extreme event which we expect to occur less frequently than every 100 years. An approximation of its return period is over 550 years. The Meteorological Data Report shows the minimum pressure of Hurricane Sandy was 945 hPa. This value also shows that the hurricane Sandy is an event we expect to occur less frequently than every 100 years. An approximation of its return period is over 1000 years. Wilks(2011) provided the annual maxima of daily precipitation amounts at Charleston, South Carolina, 1951-1970. The return period obtained using this method is the same as the result provided by Wilks (2011).

Estimating the return period of Hurricane Sandy using different methods and factors may obtain different results. Lin et al. (2012) applied a model-based risk assessment methodology and investigated the hurricane storm surge risk of New York City. They generated large numbers of synthetic storms that pass within 200 km of The Battery over the Atlantic Ocean basin, and simulate surge events around the New York area using the SLOSH model. They generated 5,000 NY-region storms under the observed climate estimated from NCEP-NCAR reanalysis. They fitted the generalized Pareto distribution (GPD) with surge distribution. The estimated 100-yr surge is about 1.74m and the estimated 500-yr surge is about 2.78m.

Shrestha et al. (2014) estimated the storm surge return period for Hurricane Sandy. The hurricane storm surge risk assessment methodology discussed in this paper is based on a statistical hurricane model and hydrodynamic models SLOSH and ADCIRC. They carried out statistical analysis to estimate the probability density function (PDF) of storm surge height and combined the PDF of storm surge heights with the annual storm frequency which can be estimated from hurricane model. They estimated return period of storm surge for Hurricane

Sandy which equals to 2.87 m s is 650 years with 95% confidence falling between 522 and 881 years.

Brandon et al. (2014) estimated the return period of hurricane Sandy's storm tide which equals to 3.4m. The estimated return period is ranging from 900 and 1600 years. They calculated the probability that event like Hurricane Sandy could occur during the last century using the formula

$$P = \frac{n!}{x!(n-x)!} p^x q^{n-x}$$

where n is the interval of time under consideration, x is number of occurrences of the event, p is probability of "success" (the event happens) and q is the probability of "failure" (the event doesn't happen).

f) Distance from The Battery to Storm Center and Storm Surge

The distance from The Battery to storm center may be considered as a factor that affects the storm surge. To verify this assumption, the distance is calculated and correlated with storm surge. The correlations between the distance from The Battery to storm center and storm surge in the blue ellipse and the red ellipse are -0.15 and -0.16, respectively. Since both values show no statistical significance at 5% significance level, the result suggests that the distance from The Battery to storm center does not have impact on surge level at The Battery.

g) Wind Velocity, Wind Stress at The Battery and Storm Surge

The wind data used in this section is the NECP-NCAR Reanalysis data from 1948 to 2012, October to March. Pick out the u-wind and v-wind data at 10 meter at The Battery when the storms are moving within the elliptical regions, and correlated them with corresponding storm surge data. For the blue ellipse, the correlation coefficients between u-wind or v-wind at The

Battery and storm surge are 0.06 and 0.28, respectively. For the red ellipse, the correlation coefficients are 0.01 and 0.25, respectively. From above results, v-wind has more impact on the storm surge compared to u-wind. In addition, correlations between wind velocity prior to surge and storm surge are calculated. The time lags of wind are 6 hour, 12 hour, 18 hour and 24hour before storm surge. Results are shown in Figure 8. From Figure 8, the correlation is the highest at Lag 0, which means wind impacts surge the most at the time that storms are moving inside the elliptical regions.

According to Talley et al. (2011), "storm surge is dependent on wind stress". Following this conclusion, correlations between storm surge and the u-wind stress and v-wind stress at The Battery are calculated. Correlations between the u-wind stress, v-wind stress and surge are equal to -0.01 and -0.07 for the blue ellipse and -0.04 and -0.07 for the red ellipse. Correlations between surge and wind stress at different time lags are shown in Figure 9. According to Figure 9, the u-wind stress has higher correlations with surge compared to v-wind stress. Wind stress 18 hours prior to the surge has the highest correlation.

Chapter 4: Summary

The objective of this study was to provide a basis for the application of the JPM method to assess the impact of extra tropical storms in the NY-NJ coastal region. I investigated storms in the historical data base using two data sets: the climate forecast system reanalysis (CFSR; Saha et al. 2010) data from 1979-2005 (November to March) and the NCEP-NCAR reanalysis data from 1948-2012 (October to March). In both studies, the following factors were investigated: storm velocity, acceleration, orientation of storms and the central pressure. Correlations between storm properties and surge suggest that storm velocity and central pressure have significant

impact on surge and lower velocity or central pressure correspond to higher surge. However, there is no evidence that acceleration has significant impact on surge.

Extreme-value analysis on maximum storm surge and minimum pressure were carried out and their 100-year return periods were calculated to estimate the probability of an unusually large event. The maximum storm surge of the hurricane Sandy measured at The Battery, New York was 2.86m and its return period from the extreme value analysis is about 550 years. Sandy's minimum pressure at The Battery was 945 hPa, and return period is over 1000 years.

The majority of storms that influence surge at The Battery travel in the northeast direction. An investigation of the relationship between the direction of the storm and surge showed that storms moving to the southeast have the highest impact on the surge.

In addition, the distance between storm center and The Battery is considered as a possible variable which impacts storm surge. However, since the correlations are not statistically significant, we can conclude that the distance from The Battery to storm center does not have impact on surge level.

Relations between wind velocity, wind stress at The Battery and storm surge were also investigated. The wind data used in this section is the NECP-NCAR Reanalysis data from 1948 to 2012, October to March at The Battery. Results show that v-wind has more impact on the storm surge compare to u-wind. The correlation between wind and surge is the highest at Lag 0, which means wind impacts surge the most at the time that storms are inside the elliptical regions. For wind stress and surge, results show that the u-wind stress has higher correlations with surge compared to v-wind stress, and wind stress 18 hours prior to the surge has the highest correlation.

The results obtained in this thesis suggest that 95% of cyclone features that generate a surge at The Battery, New York are over the elliptical regions shown in Figure 2. The storms

responsible for the strongest surges have below average velocities and below average central pressures while in these regions. Most of the storms travel towards the northeast in the regions but the minority that move from the northwest to the southeast have the strongest impact on surge at Battery, New York.

References:

Bowman, M. J., B. A. Colle, R. Flood, D. Hill, R. E. Wilson, F. Buonaiuto, P. Cheng, and Y. Zheng, 2005:Hydrologic feasibility of storm surge barriers to protect the metropolitan New York–New Jersey region: Final report. Marine Sciences Research Center Tech. Rep., Stony Brook University, 28 pp.

Blake, E., Kimberlain, T., Berg, R., Cangialosi, J., Beven., 2012: Tropical Cyclone Report Hurricane Sandy, National Hurricane Center.
http://www.nhc.noaa.gov/data/tcr/AL182012_Sandy.pdf

Brandon, C.M., Woodruff, J.D., Donnelly, J.P. & Sullivan, R.M., 2014: How Unique was Hurricane Sandy? Sedimentary Reconstructions of Extreme Flooding from New York Harbor. Sci. Rep. 4, 7366; DOI:10.1038/srep07366.

Chang, E. K. M., 2014: Impacts of background field removal on CMIP5 projected changes in Pacific winter cyclone activity. J. Geophys. Res. Atmos., 119, 4626-4639.

Chanson, H., 2004: Environmental Hydraulics for Open Channel Flows, 1st Edition. Butterworth-Heinemann

Colle, B.A., Buonaiuto, F., Bowman, M.J., Wilson, R.E., Flood, R., Hunter, R., Mintz, A., Hill, D., 2008: New York City's vulnerability to coastal flooding. *Bull. Amer. Met. Soc*. 89, 829-841

Colle, B. A., K. Rojowsky, and F. Buonaiuto, 2010: New York City storm surges: 648 Climatology and analysis of the wind and cyclone evolution. J. Appl. Meteor. and 649 Climatology, 49, 85-100.

Colle, B., Z. Zhang, K.Lombardo, E. Chang， P.Liu, and M. Zhang, 2013: Historical evaluation and future prediction of eastern North America and western Atlantic extratropical cyclones in the CMIP5 models during the cool season. J. Climate. Doi:10.1175/JCLI-D-12-00498, in press.

Extratropical Storm Surge, http://www.mahalo.com/extratropical-storm-surge/.
Fanelli, C., P. Fanelli and D.Wolcott, 2013: Hurricane Sandy. NOAA Water Level and Meteorological Data Report

Federal Emergency Management Agency (FEMA), 2008. Mississippi Coastal Analysis Project. Project reports prepared by URS Group Inc., (Gaithersburg, MD and Tallahassee, FL) under HMTAP Contract HSFEHQ-06-D-0162, Task Order 06-J-0018.

Federal Emergency Management Agency (FEMA), 2012. Joint Probability – Optimal Sampling Method for Tropical Storm Surge Frequency Analysis. Operating Guidance No. 8-12.

Granthem, K. N., 1953. "Wave Run-up on Sloping Structures". *Transactions of the American Geophysical Union* **34** (5): 720-724. doi:10.1029/tr034i005p00720. 21

Harris, D.L. ,1963: "Characteristics of the Hurricane Storm Surge" (PDF). *Technical Paper No. 48* (Washington, D.C.: U.S. Dept. of Commerce, Weather Bureau): 1–139.
Hodges, K. I., 1999: Adaptive constraints for feature tracking, Mon. Weather Rev., 127,1362-1373.

Hawks, P., 2005: "Use of Joint Probability Method in Flood Management: A Guide to Best Practice". Defra/Environment Agency R&D Technical Report FD2308/TR2.

Ho, F.P., Myers V.A., 1975: "Joint Probability Method of Tide Frequency Analysis applied to Apalachicola Bay and St. George Sound, Florida", NOAA Tech. Rep. WS 18, 43 p.

Hodgesm K.I. 1994: A General Method for Tracking Analysis and its Application to Meterological Data, Mon. Weather Rev., V122, 2573-2586.

Hodges, K. I., 1995: Feature tracking on the unit sphere. Mon. Wea. Rev., 123, 3458–3465

Hodges, K. I., 1999: Adaptive constraints for feature tracking, Mon. Weather Rev., 127,1362-1373.

Kantha, L. H., C. Tierney, J. W. Lopez, S. D. Desai, 1994: The inverted barometer effect in altimetry: A study in the North Pacific. TOPEX/Poseidon Res. News 2, 18–23.

Lin, N., Emanuel, K. A., Oppenheimer, M., and Vanmarke, E., 2012: "Physically Based Assessment of Hurricane Surge Under Climate Change." *Nature Climate Change*, 2(6), 1-6.

Myers, V.A., 1975: "Storm Tide Frequencies on the South Carolina Coast", NOAA Tech. Rep. NWS-16, 79 p.

National Hurricane Center, "Introduction to Storm Surge".
http://www.nws.noaa.gov/om/hurricane/resources/surge_intro.pdf

Niedoroda, A.W., D.T. Resio, G.R. Toro, D. Divoky, H. Das, and C.W. Reed 2010: "Analysis of the coastal Mississippi storm surge hazard," *Ocean Engineering,* Vol. 37, No. 1, pp. 82-90.

Resio, D.T., 2007: "Estimating Hurricane Inundation Probabilities." White paper for US Army Corps of Engineers, ERDC-CHL. May 7, 2007.

Saha, S., and Coauthors, 2010: The NCEP Climate Forecast System Reanalysis. Bull. 747 Amer. Meteor. Soc., 91, 1015–1057.

Sheng, Y. P., V. Alymov, and V. A. Paramygin 2010: Simulation of storm surge, wave, currents, and inundation in the Outer Banks and Chesapeake Bay during Hurricane Isabel in 2003: The importance of waves, J. Geophys. Res., 115, C04008, doi:10.1029/2009JC005402.

Shrestha, P., James, S., Shaller, P., Doroudian, M., Peraza, D., and Morgan, T., 2014: Estimating the Storm Surge Recurrence Interval for Hurricane Sandy. World Environmental and Water Resources Congress 2014: pp. 1906-1915.doi: 10.1061/9780784413548.191

Talley L.D., Pickard G.L., Emery W.J., Swift J.H., 2011. Descriptive Physical Oceanography: An Introduction (Sixth Edition)

Toro, G.R., A.W. Niedoroda, C.W. Reed, and D. Divoky, 2010: "Quadrature-based approach for the efficient evaluation of surge hazard," *Ocean Engineering,* Vol. 37, No. 1, pp. 114-124.

Toro, G.R., D.T. Resio, D. Divoky, A.W. Niedoroda, and C. Reed,2010b :"Effective joint-probability methods of hurricane surge frequency analysis," *Ocean Engineering,* Vol. 37, No. 1, pp. 125-134.

Weisberg RH, Zheng L, 2006: Hurricane storm surge simulations for Tampa Bay. Estuaries Coasts 29(6A):899–913

Wilks, D, 2011: Statistical Methods in the Atmospheric Sciences. Academic Press.

Appendix:

Tables:

Table 1a): Correlation coefficients between storm surge and variables obtained from CFSR reanalysis data, 1979-2005. Statistically significant correlations are shown in bold

		Velocity	Acceleration	Pressure
Blue Ellipse	Surge	**-0.32**	0.03	**-0.24**
Red Ellipse		**-0.27**	0.15	**-0.22**

Table 1b): Correlation coefficients between storm surge and variables for 1948-2012. Statistically significant correlations are shown in bold.

		Velocity	Acceleration	Pressure
Blue Ellipse	Surge	**-0.31**	-0.06	**-0.39**
Red Ellipse		**-0.22**	-0.08	**-0.36**

Table 2: Correlation coefficients between storm surge and velocity for storms moving in different directions. Statistically significant correlations are shown in bold.

Range of Angles (Degree)	Blue Ellipse		Red Ellipse	
	Correlation	Num. of Storm	Correlation	Num. of Storm
-90~-45	-0.27	8	-0.44	7
-45~0	**-0.31**	151	**-0.32**	176
0~20	**-0.18**	452	**-0.18**	480
20~40	**-0.22**	478	**-0.23**	544
40~60	-0.17	170	-0.09	193
60~80	-0.12	38	-0.09	27

Figures:

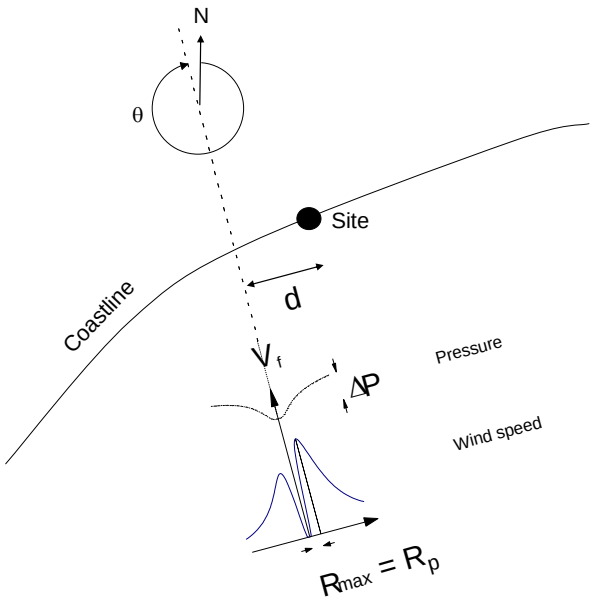

Figure 1: Storm characteristics described by the JPM method.

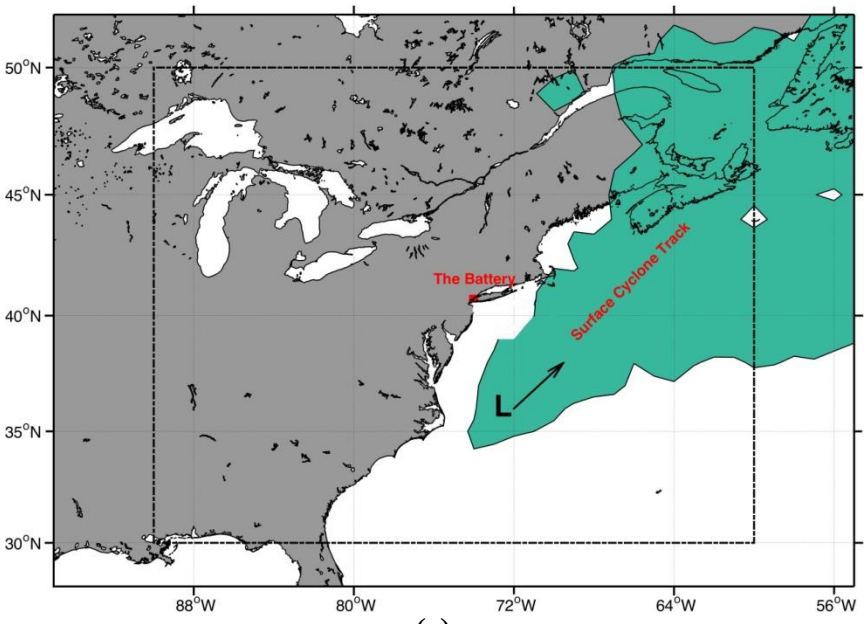

(a)

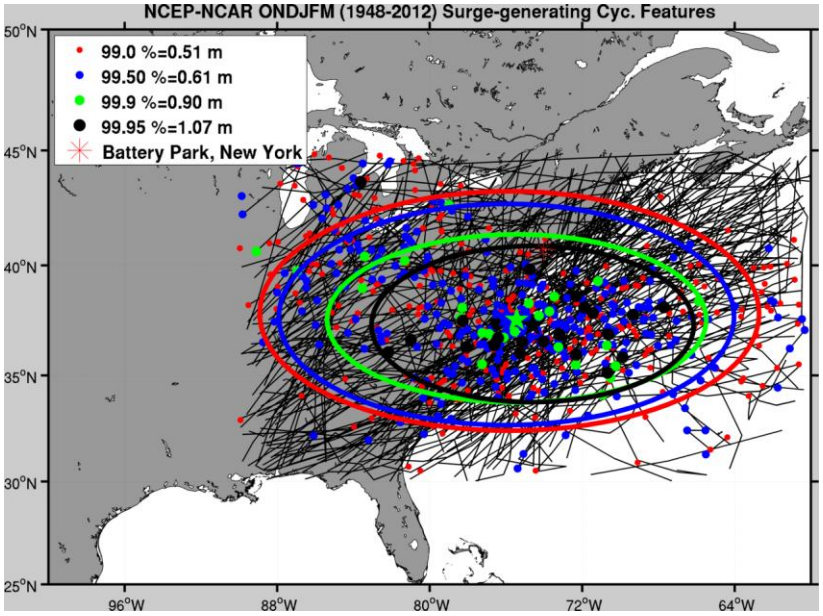

(b)

Figure 2: Surge-generating cyclone tracks for 1948-2012, October to March. Cyclone tracks are paired with Battery Park's surge record. Figure 2a: the black box contains all cyclones that generate surge; Figure 2b: The color code in the legend indicates the elliptical regions containing storm tracks associated with the surge at The Battery greater than or equal the stated percentile of surges. 95% of all cyclones that generate the surge at The Battery occur within the elliptical regions.

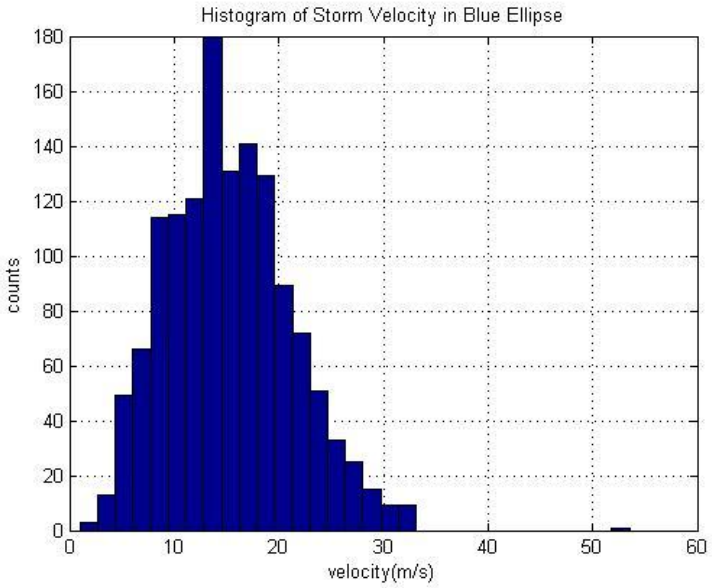
Histogram of Storm Velocity in Blue Ellipse
counts
velocity(m/s)
0
20
40
60
80
100
120
140
160
180
0
10
20
30
40
50
60

(a)

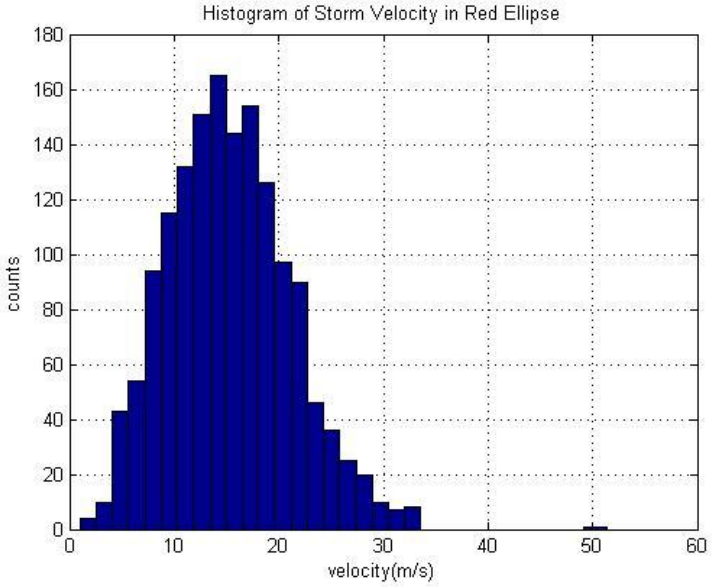
Histogram of Storm Velocity in Red Ellipse
counts
velocity(m/s)
0
20
40
60
80
100
120
140
160
180
0
10
20
30
40
50
60

(b)

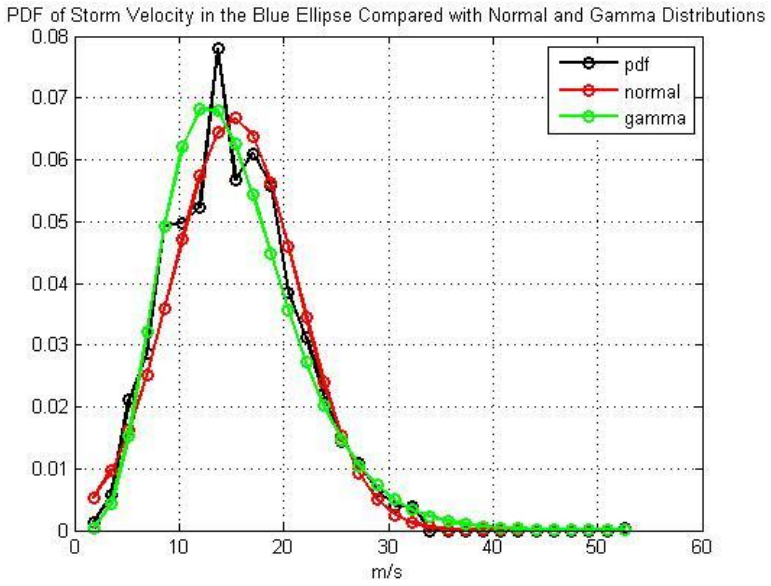
PDF of Storm Velocity in the Blue Ellipse Compared with Normal and Gamma Distributions
pdf
normal
gamma
0.08
0.07
0.06
0.05
0.04
0.03
0.02
0.01
0
0
10
20
30
40
50
60
m/s

(c)

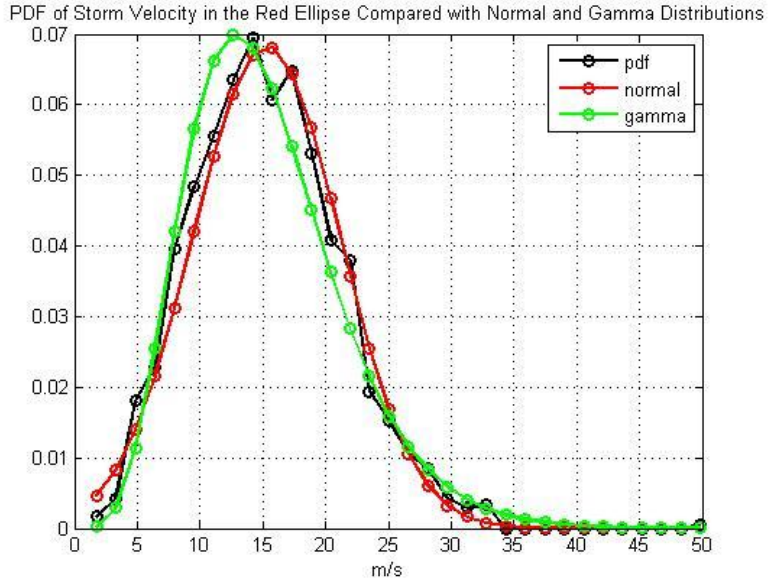
PDF of Storm Velocity in the Red Ellipse Compared with Normal and Gamma Distributions
pdf
normal
gamma
0.07
0.06
0.05
0.04
0.03
0.02
0.01
0
0
5
10
15
20
25
30
35
40
45
50
m/s

(d)

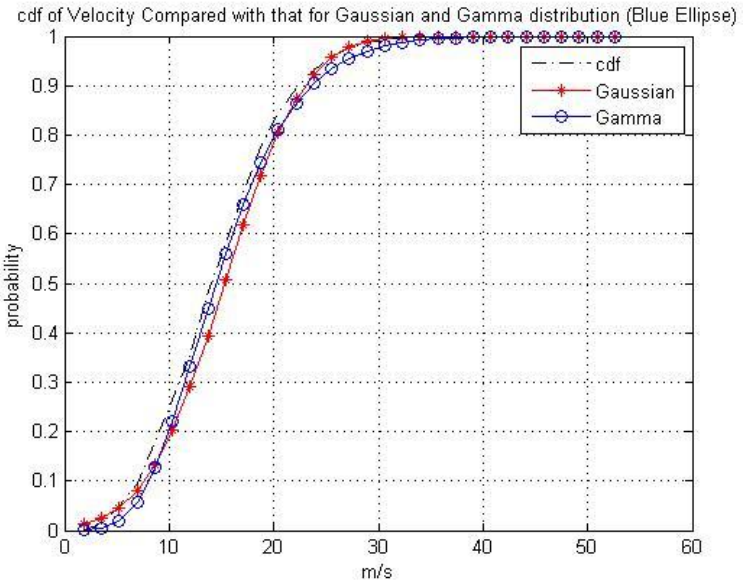

(e)

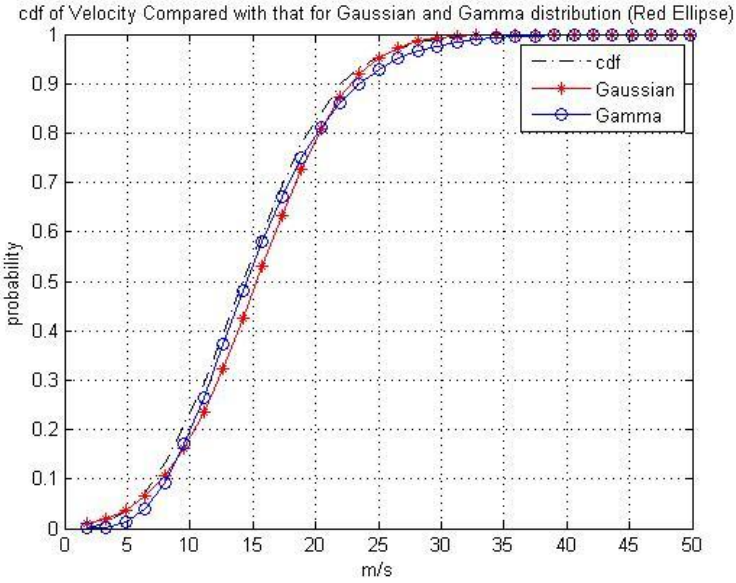

(f)

Figure 3: Histogram of storm velocity (a): blue ellipse; (b) red ellipse.
Probability density function of storm velocity in the blue ellipse (c) and the red ellipse (d) compare with Gaussian and Gamma distribution. Cumulative distribution function of storm velocity in the blue ellipse (e) and the red ellipse (f) compare with Gaussian and Gamma distribution.

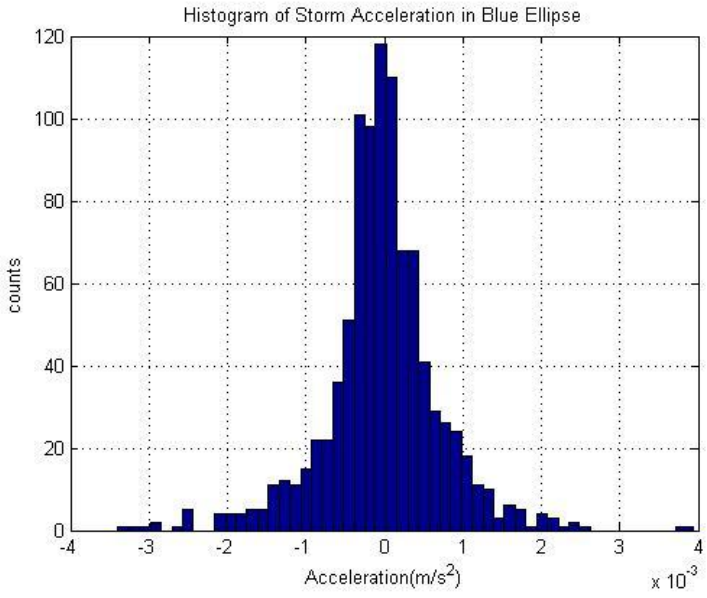
Histogram of Storm Acceleration in Blue Ellipse
counts
Acceleration(m/s^2)
x 10^{-3}

(a)

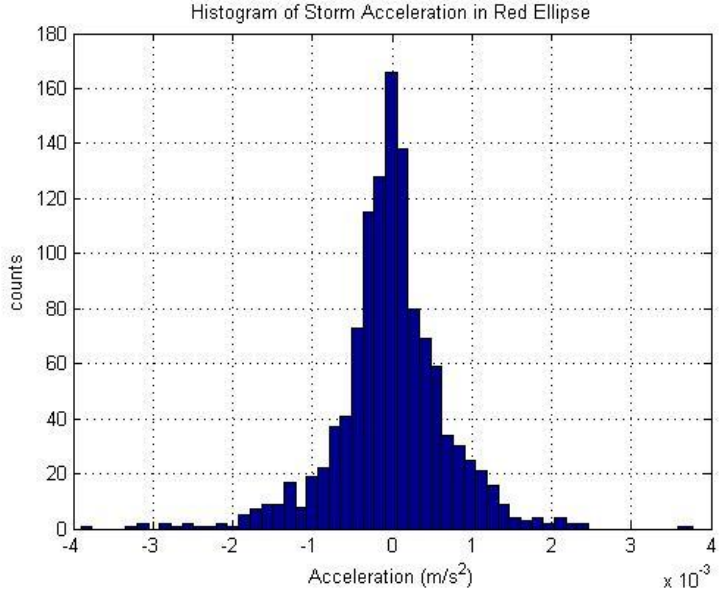
Histogram of Storm Acceleration in Red Ellipse
counts
Acceleration (m/s^2)
x 10^{-3}

(b)

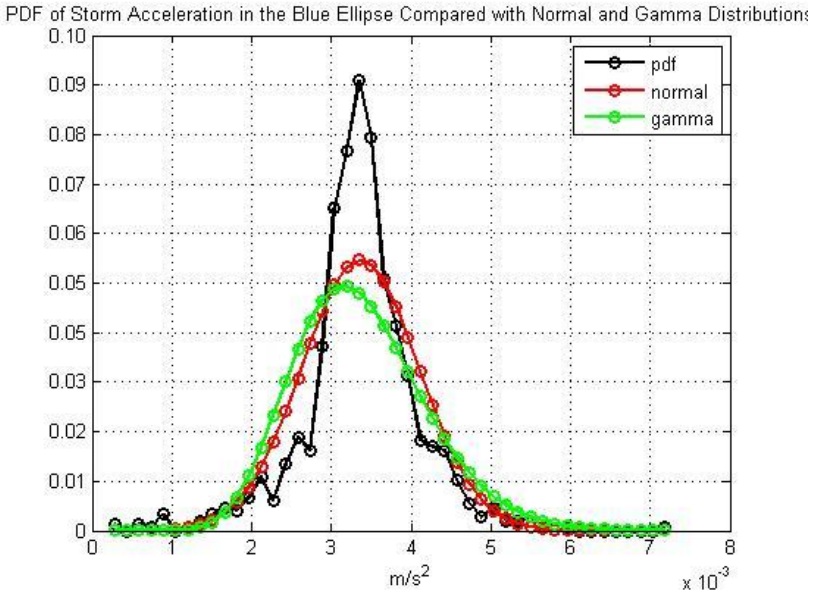

(c)

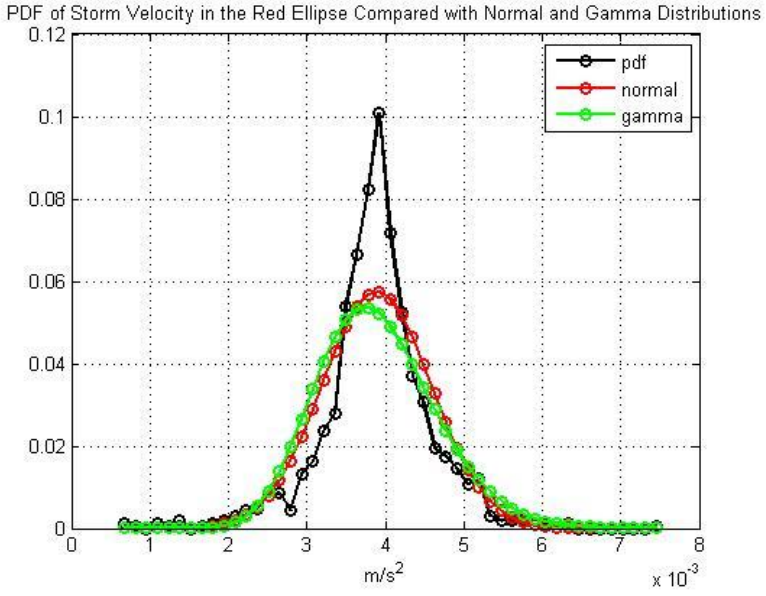

(d)

Figure 4: Histogram of storm acceleration (a): blue ellipse; (b) red ellipse.
Probability density function of storm acceleration in the blue ellipse (c) and the red ellipse (d) compare with Gaussian and Gamma distribution.

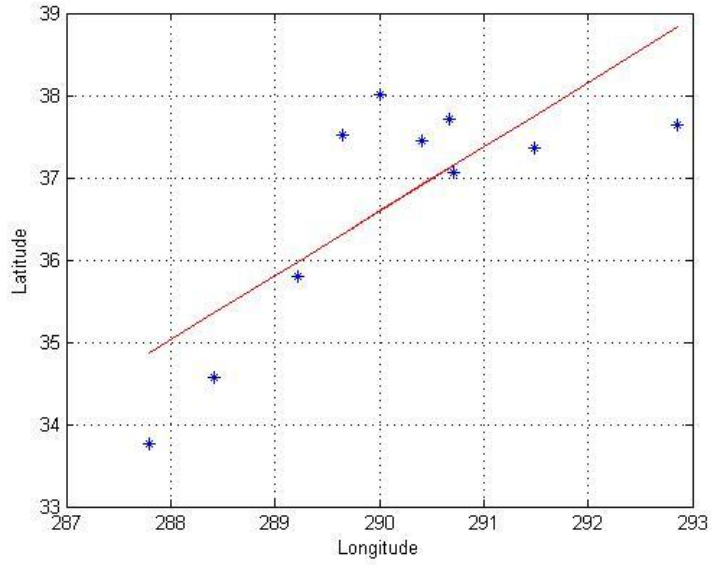
39
38
37
36
35
34
33
Latitude
287
288
289
290
291
292
293
Longitude

(a)

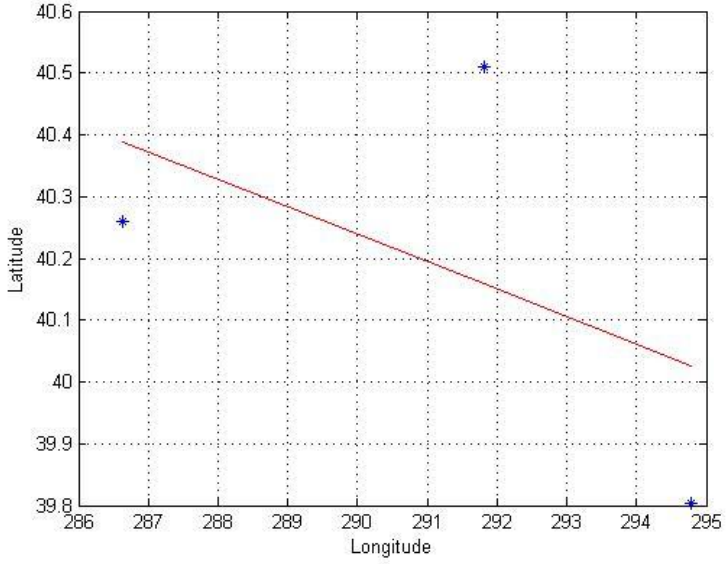
40.6
40.5
40.4
40.3
40.2
40.1
40
39.9
39.8
Latitude
286
287
288
289
290
291
292
293
294
295
Longitude

(b)

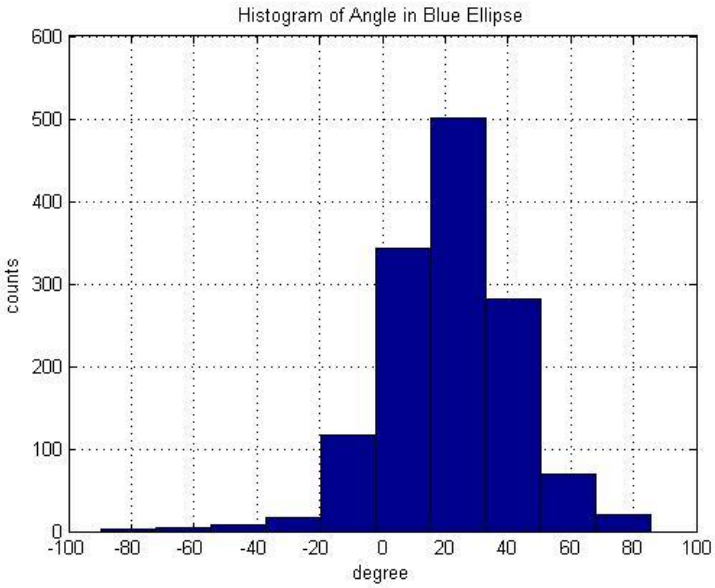

(c)

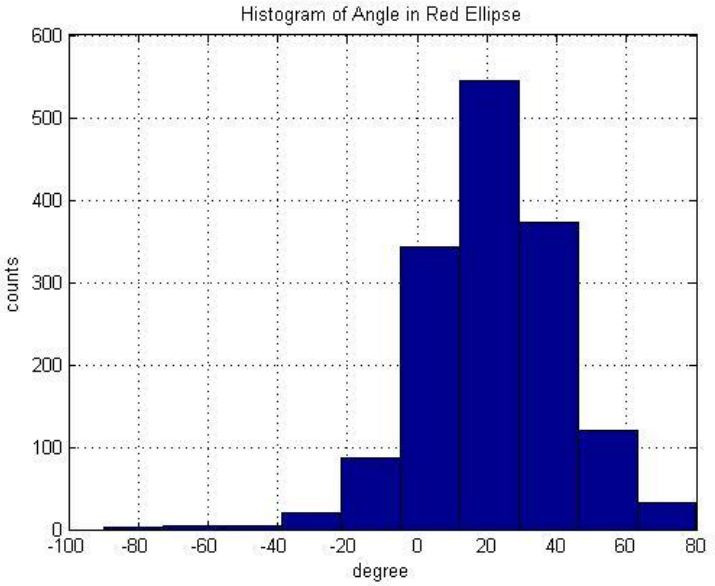

(d)

Figure 5: Eliminated storm examples when calculating the orientations are shown in panels (a) and (b). Blue stars are the location of storm at each time step. Red line is the moving track predicted by linear regression. Panels (c) and (d) are the histograms of storm angles for blue ellipse and red ellipse.

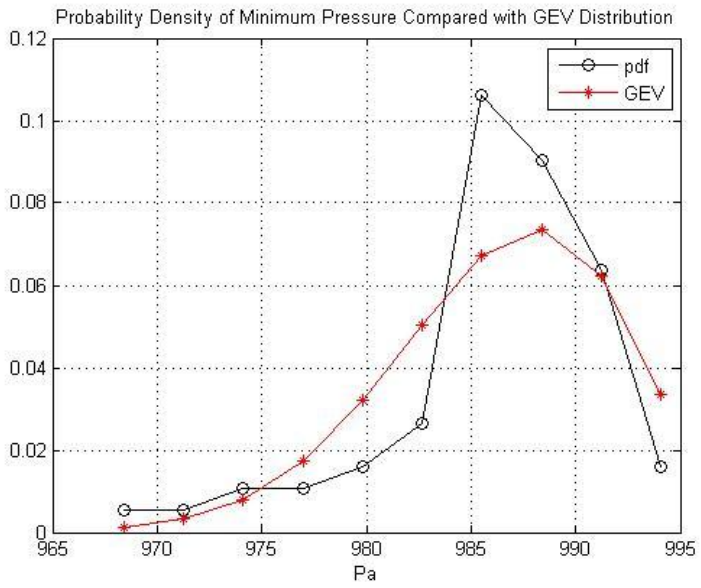

(a)

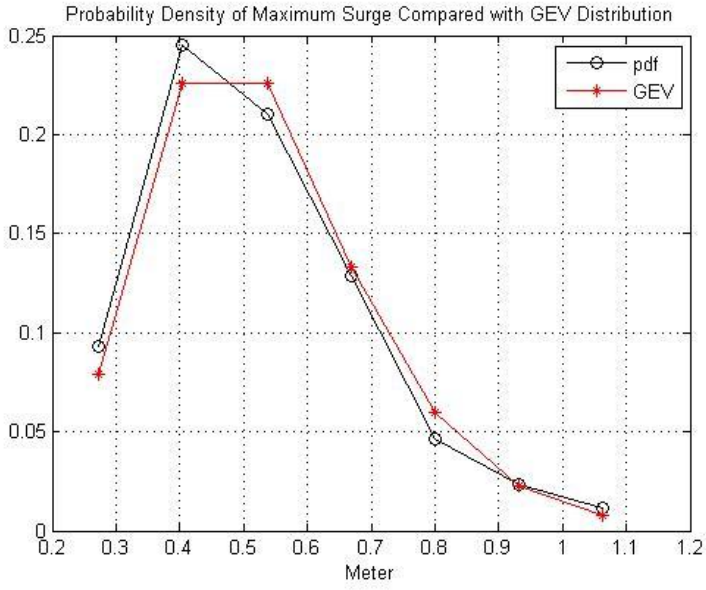

(b)

Figure 6: Probability density function of (a) minimum pressure and (b) maximum storm surge compared with their fitting to the extreme value distribution

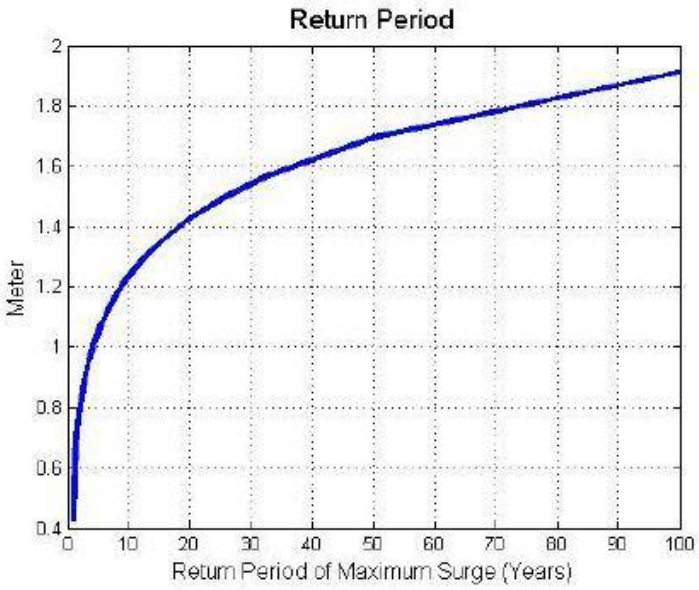

(a)

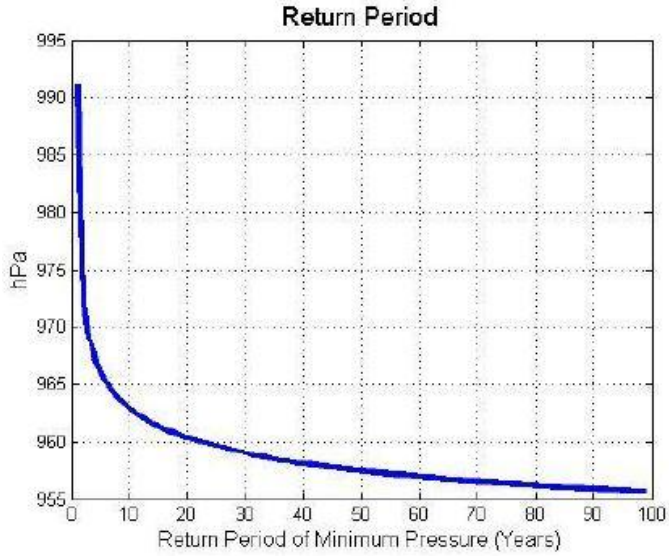

(b)

Figure 7: 100-year return period of: (a) maximum storm surge (b) and minimum pressure

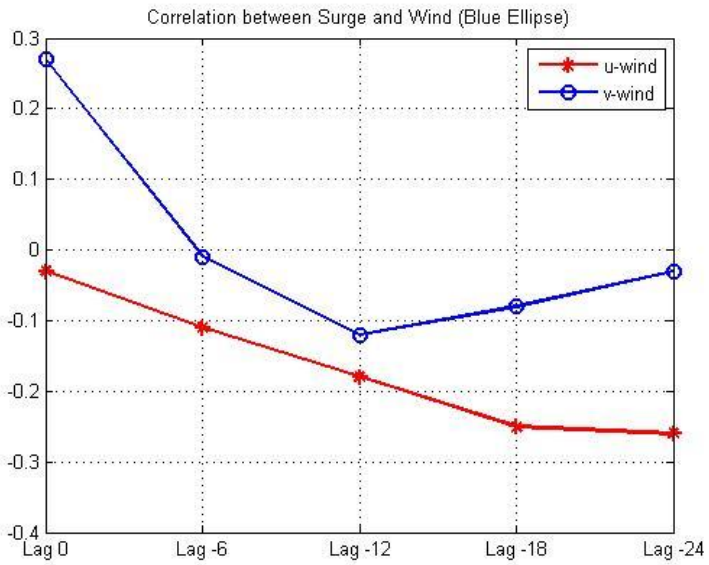

(a)

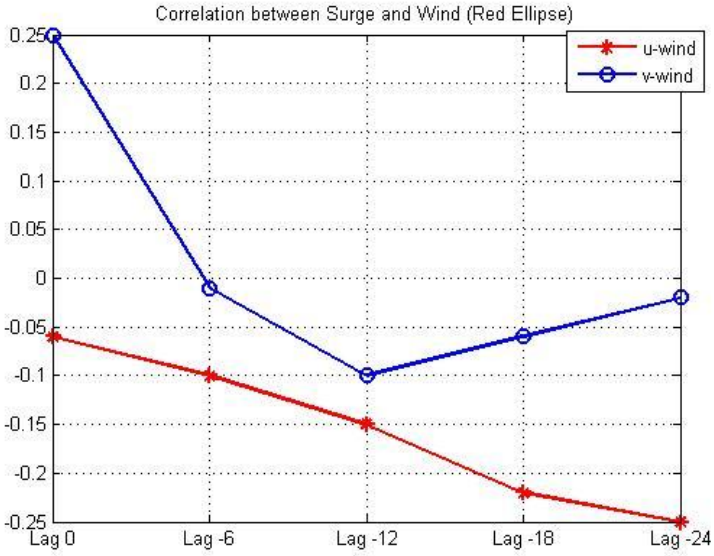

(b)

Figure 8: Correlation between surge and wind for a) blue ellipse; b) red ellipse. Lag -6, Lag -12 etc represent 6, 12 etc hours before the storm.

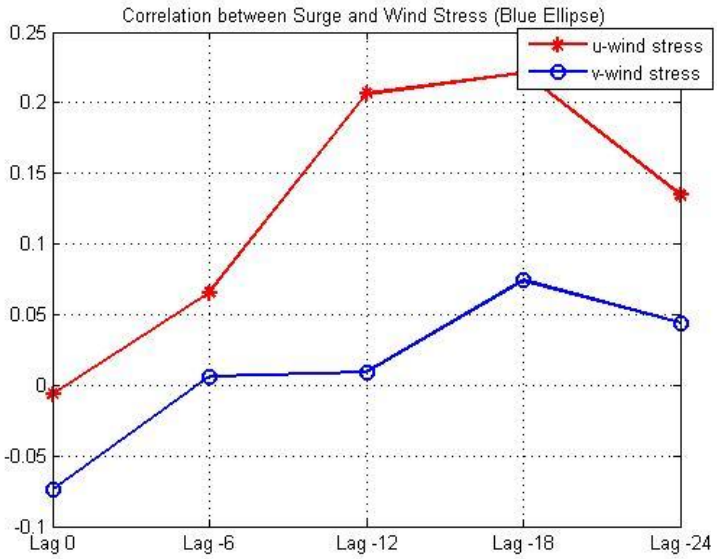

(a)

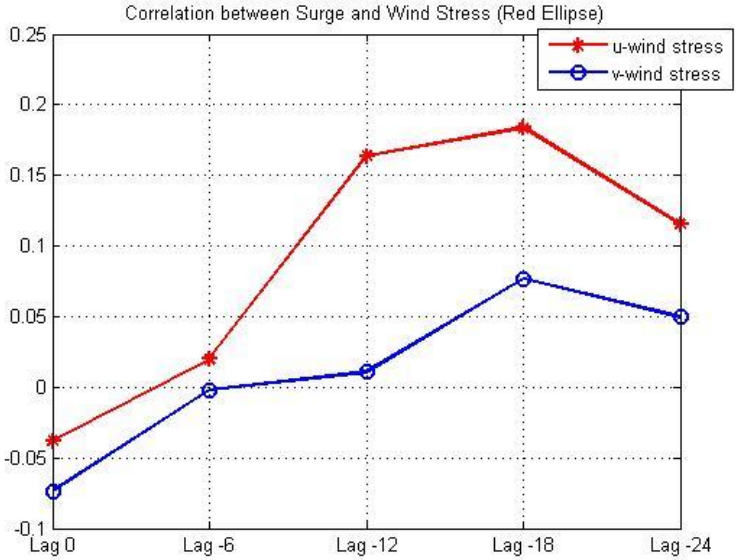

(b)

Figure 9: Correlation between surge and wind stress for a) blue ellipse; b) red ellipse. Lag -6, Lag -12 etc represent 6, 12 etc hours before the storm.